

# Mitigating murine acute and chronic Coxsackievirus B3-induced myocarditis with human right atrial appendage-derived stromal cells

Muhammad El-Shafeey<sup>1,2,3</sup>, Kathleen Pappritz<sup>1,2</sup>, Isabel Voss<sup>1,2</sup>, Kapka Miteva<sup>1,4</sup>, Alessio Alogna<sup>2,5</sup>, Martina Seifert<sup>1,2,6</sup>, Henry Fechner<sup>7</sup>, Jens Kurreck<sup>7</sup>, Karin Klingel<sup>8</sup>, Marion Haag<sup>1,9</sup>, Michael Sittlinger<sup>1,9</sup>, Carsten Tschöpe<sup>1,2,5</sup>, Sophie Van Linthout<sup>1,2,\*</sup>

<sup>1</sup>Berlin Institute of Health (BIH) at Charité – Universitätsmedizin Berlin, BIH Center for Regenerative Therapies (BCRT), 13353 Berlin, Germany

<sup>2</sup>DZHK (German Center for Cardiovascular Research) Partner Site, Berlin, Germany

<sup>3</sup>Medical Biotechnology Research Department, Genetic Engineering and Biotechnology Research Institute (GEBRI), City of Scientific Research and Technological Applications, 21934 Alexandria, Egypt

<sup>4</sup>Division of Cardiology, Foundation for Medical Research, Department of Medicine, Faculty of Medicine, University of Geneva, 1211 Geneva, Switzerland

<sup>5</sup>Deutsches Herzzentrum der Charité (DHZC), Department of Cardiology, Angiology and Intensive Medicine, Campus Virchow Klinikum, 13353 Berlin, Germany

<sup>6</sup>Institute for Medical Immunology, Charité – Universitätsmedizin Berlin, Corporate Member of Freie Universität Berlin and Humboldt Universität zu Berlin, 13353 Berlin, Germany

<sup>7</sup>Institute of Biotechnology, Chair of Applied Biochemistry, Technische Universität Berlin, 13355 Berlin, Germany

<sup>8</sup>Cardiopathology, Institute for Pathology and Neuropathology, University Hospital Tübingen, 72074 Tübingen, Germany

<sup>9</sup>Tissue Engineering Laboratory, Charité-Universitätsmedizin Berlin, Corporate Member of Freie Universität Berlin, Humboldt-Universität zu Berlin, and Berlin Institute of Health, 10117 Berlin, Germany

\*Corresponding author: Sophie Van Linthout, PhD, Translational Immunocardiology, Berlin Institute of Health at Charité – Universitätsmedizin Berlin, BIH Center for Regenerative Therapies (BCRT), Föhrer Strasse 15, 13353 Berlin, Germany ([sophie.van-linthout@bih-charite.de](mailto:sophie.van-linthout@bih-charite.de)).

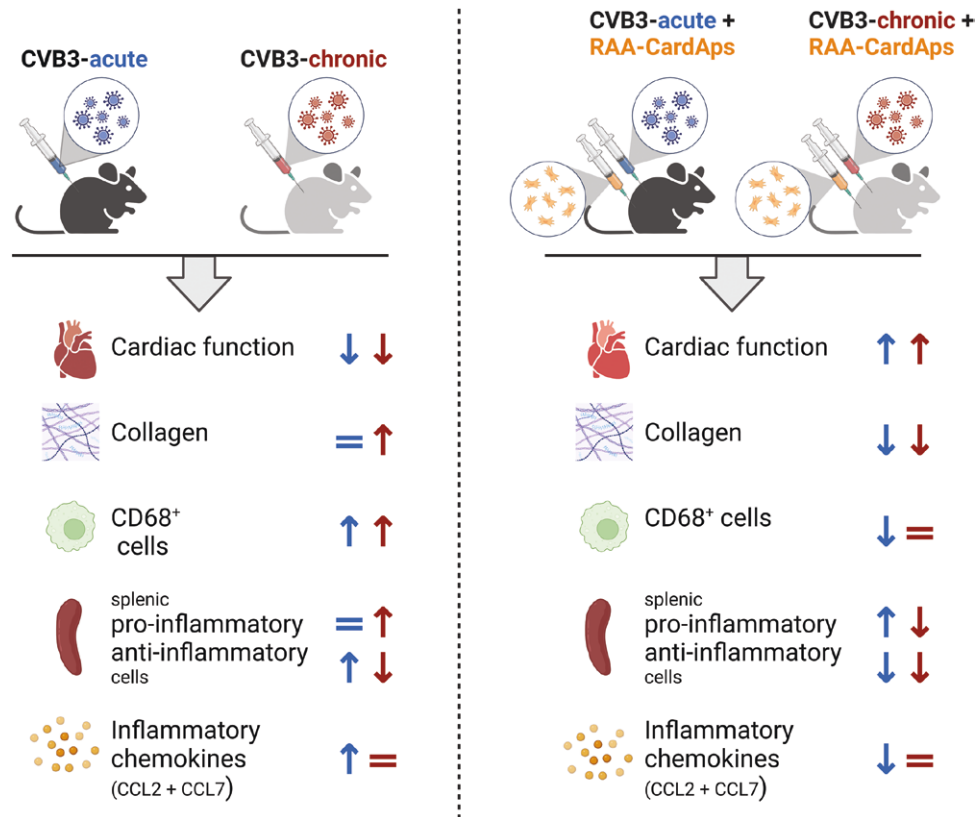
## Abstract

We previously have shown the potential of human endomyocardial biopsy (EMB)-derived cardiac adherent proliferating cells (CardAPs) as a new cell-therapeutic treatment option for virus-induced myocarditis. To overcome the limited cell yield per EMB, CardAPs have been isolated from the human right atrial appendage (RAA) in view of allogeneic application and off-the-shelf use. We aimed to investigate the cardioprotective and immunomodulatory potential of RAA-CardAPs in experimental acute and chronic Coxsackievirus B3 (CVB3)-induced myocarditis upon injection in the viral and inflammatory phase. In the acute model, male C57BL/6J mice were intraperitoneally (i.p.) injected with the CVB3 Nancy strain or phosphate buffered saline (PBS). One day after infection, mice were intravenously (i.v.) injected with RAA-CardAPs, EMB-CardAPs (as reference cells) or PBS. For the chronic model, male Naval Medical Research Institute mice were i.p. injected with the CVB3 31-1-93 strain or PBS. Ten days after infection, mice were i.v. injected with RAA-CardAPs. Cardiac function was characterized, followed by harvest of the left ventricle (LV) and spleen for subsequent analysis, 7 and 28 days after CVB3 infection in the acute and chronic model, respectively.

In the acute model, RAA-CardAPs decreased cardiac fibrosis and improved cardiac function in CVB3 mice. RAA-CardAPs mice exerted immunomodulatory effects as evidenced by lower LV chemokines expression (C-C motif ligand [CCL]2 and CCL7), CD68<sup>+</sup> cells presence, intercellular adhesion molecule-1, vascular cell adhesion molecule-1, tumor necrosis factor- $\alpha$ , and IL-6 mRNA expression. In the chronic model, RAA-CardAPs reduced cardiac fibrosis and the severity of myocarditis, associated with an improvement in LV function. We conclude that RAA-CardAPs represent a treatment strategy to reduce the development of acute and chronic CVB3-induced myocarditis.

**Key words:** cardiac stromal cells; Coxsackievirus B3; myocarditis.

## Graphical abstract



### Significance statement

Coxsackievirus B3 (CVB3) infection is an important cause of myocarditis, an inflammatory cardiac disorder for which no target-specific treatment options are currently available. We previously have shown the potential of human endomyocardial biopsy (EMB)-derived cardiac adherent proliferating cells (CardAPs) as a new cell-therapeutic treatment option for virus-induced myocarditis. To overcome the limited cell yield per EMB, we isolated CardAPs from the human right atrial appendage (RAA) in view of allogeneic application and off-the-shelf use. Our study shows the therapeutic efficacy of intravenous RAA-CardAPs application for acute and chronic CVB3 myocarditis.

## Introduction

Myocarditis is an inflammatory cardiac disease, primarily caused upon viral infection.<sup>1,2</sup> From the broad spectrum of viruses,<sup>1,3</sup> particularly infections with Coxsackievirus B3 (CVB3) are a known cause of acute viral myocarditis in young, otherwise healthy patients.<sup>4</sup> The prevalence of myocarditis has been reported to be between 10.2 and 105.6 per 100 000 worldwide, with an estimated annual incidence of around 1.8 million cases.<sup>5</sup> Despite enormous advances in diagnosis and understanding of the underlying pathogenesis of viral myocarditis, no target-specific treatment options are currently available.<sup>6</sup> Patients are treated with conventional heart failure medication, treating the symptoms rather than the underlying cause of the disease.<sup>6</sup> A significant proportion of patients eventually develop dilated cardiomyopathy, resulting in end-stage heart failure, where heart transplantation is the only treatment option,<sup>1,6</sup> indicating the need for alternative options.

Since pioneering preclinical research on the use of cell therapy for cardiac regeneration in the last quarter of the 20th century, many novel insights have been gathered and advances have been made in the 21st century, making this still

a relatively young field.<sup>7</sup> Different cell types have been used so far, including cardiac stem cells<sup>8</sup> and mesenchymal stromal cells (MSC).<sup>9</sup> Meanwhile, it is well accepted that the improvement in cardiac function following administration of most cell types is primarily due to paracrine effects, stimulating endogenous cardiac repair.<sup>9-12</sup> Further evidence with MSC states the relevance of their immunomodulatory effects inducing both local cardiac and systemic inflammatory changes.<sup>9,13,14</sup> However, the translation from preclinical research to the bedside has not maintained all the initial promises, accentuating the need for further refinement of cell therapy, ranging from the cell product itself towards the method and time of delivery. In fact, one of the main challenges of cell therapy is that cells need to be easily isolated and expanded, enabling their use in the needed therapy window.<sup>15</sup>

CardAPs are isolated from human EMB,<sup>16</sup> and share the main characteristics of MSC.<sup>17</sup> They are non-hematopoietic cells, adhere to plastic, and express CD73, CD105, and CD166. However, they do not have the multi-lineage property.<sup>16</sup> EMB-CardAPs display low immunogenicity in the presence or absence of inflammatory conditions.<sup>17</sup> They further have anti-apoptotic,<sup>18</sup> anti-fibrotic,<sup>19</sup> and immunomodulatory properties,<sup>17</sup> which have been shown to be reflected in an

improvement of left ventricle (LV) function, following their application in different experimental models.<sup>18,19</sup>

However, the number of cells, which can be isolated from 1 EMB,<sup>16</sup> is limited due to the small size of the biopsy,<sup>20</sup> highlighting the need for an alternative source in view of allogeneic application and off-the-shelf use. Therefore, CardAPs have been isolated from right atrial appendage (RAA), which allows a sufficient number of isolated cells for the treatment of more than 250 patients.<sup>20</sup> Similar to EMB-CardAPs, RAA-CardAPs are CD90<sup>low</sup> expressing cells, sharing the same characteristics,<sup>20</sup> including immunomodulatory properties.<sup>21</sup> Though, the cardioprotective potential of RAA-CardAPs has not been evaluated so far, neither the optimal timepoint of administration. Therefore, this study aimed first to characterize the cardioprotective and immunomodulatory effects of RAA-CardAPs intravenously administered in the viral phase of acute CVB3-induced myocarditis mice with EMB-CardAPs as reference cells, to next evaluate their cardioprotective and immunomodulatory potential when injected in the inflammatory phase of chronic CVB3-induced myocarditis mice.

## Materials and methods

### Isolation and expansion of endomyocardial biopsy-derived cardiac adherent proliferating cells

Donation of cardiac tissue was approved by the ethical committee of the Charité-Universitätsmedizin Berlin (No 225-07) and by the patients, who provided written consent. As described by Haag *et al.*,<sup>16</sup> EMB were obtained from patients without symptoms and signs of congestive heart failure but suffering from atypical chest complaints in a standardized manner to exclude the existence of cardiomyopathy after routine noninvasive diagnostic work-up and angiography had failed to identify any specific cause of heart failure. EMB-CardAPs were isolated from the EMB by outgrowth culture from the EMB and expanded in 1/3 IMDM, 1/3 DMEM, and 1/3 Ham's F12 medium, supplemented with 5% human allogenic serum, 1% penicillin/streptomycin (Biochrom, Berlin, Germany), 20 ng/mL basic fibroblast growth factor (bFGF), and 10 ng/mL epidermal growth factor (EGF).<sup>16</sup> Cells were passaged until passage 4 for subsequent in vivo experiments.

### Isolation and expansion of right atrial appendage-derived cardiac adherent proliferating cells

Donation of cardiac tissue was approved by the ethical committee of the Charité-Universitätsmedizin Berlin (No 4/028/12) and by the patients, who provided written consent. As previously described by Detert *et al.*,<sup>20</sup> RAA were obtained from patients undergoing heart surgery at the Deutsches Herzzentrum Berlin, now Deutsches Herzzentrum der Charité (DHZC). RAA-CardAPs were isolated by outgrowth culture from the RAA. In brief, isolated CD90<sup>low</sup> RAA-CardAPs were expanded under standard cell culture conditions in full medium comprising 1/3 IMDM, 1/3 DMEM, and 1/3 Ham's F12 medium, supplemented with 5% human allogenic serum, 1% penicillin/streptomycin (Biochrom, Berlin, Germany), 100 ng/mL bFGF and 100 ng/mL EGF. Cells were propagated until passage 4 for subsequent in vivo experiments.

### Animals

All mice were purchased from Charles River (Sulzfeld, Germany) and housed in the animal facilities of the Charité – Universitätsmedizin Berlin under standard housing conditions

(12 hours light/dark cycle, 50%-70% humidity, 19-21 °C). Animals were housed with 4-5 mice per cage with unlimited access to food and water and allowed to acclimate for 2 weeks. All experiments were performed according to the European legislation for the Care and Use of Laboratory Animals (Directive 2010/63/EU) and approved by the local ethics committee (Landesamt für Gesundheit und Soziales, Berlin, G0094/11 for the acute CVB3 myocarditis model and G0186/15 for the chronic CVB3 myocarditis model).

### Coxsackievirus B3-induced acute myocarditis mice

Eight-weeks old male C57BL6/J mice were randomly divided into 4 groups: control, CVB3, CVB3 + RAA-CardAPs, and CVB3 + EMB-CardAPs, with  $n = 5$  per group. To induce viral myocarditis, mice were i.p. injected with  $1 \times 10^5$  plaque-forming units (p.f.u.) of CVB3 (Nancy strain) in 200  $\mu$ L PBS, as described previously.<sup>22,23</sup> Control mice received the same volume of sole PBS. One day (d) after infection, mice were i.v. injected either with  $1 \times 10^6$  RAA-CardAPs or EMB-CardAPs, used as reference cells, in 200  $\mu$ L PBS or sole PBS. At day (d) 7 post-infection, cardiac function was determined by hemodynamic measurement using a conductance catheter, followed by harvest of the LV and spleen for subsequent analysis.

### Coxsackievirus B3-induced chronic myocarditis mice

Seven-week old male outbred Naval Medical Research Institute (NMRI) mice were randomly divided into 4 groups: control,  $n = 9$ , control + RAA-CardAPs,  $n = 9$ , CVB3,  $n = 17$ , and CVB3 + RAA-CardAPs,  $n = 15$ . Further details for the  $n$  number of mice used for each molecular investigation are stated in the Figure legends. To induce chronic viral myocarditis, mice were i.p. injected with  $5 \times 10^5$  p.f.u. of the CVB3 strain 31-1-93 in 200  $\mu$ L PBS, as described previously.<sup>24</sup> Control mice were injected with the same volume of sole PBS. Mice were treated either with  $1 \times 10^6$  RAA-CardAPs in PBS or with PBS injected at d10 post-infection. To determine the effect of cell application on cardiac function, mice were hemodynamically characterized at d28 post infection, followed by harvest of the LV and spleen for subsequent analysis.

### Hemodynamic characterization

To determine the effect of i.v. applied RAA-CardAPs and EMB-CardAPs on cardiac function, mice were hemodynamically characterized at d7 post-infection in the acute model or at d28 in the chronic model. Animals were anesthetized with a mixture of 1.2 g/kg body weight (BW) urethane (Sigma-Aldrich Chemie GmbH, Steinheim, Germany) and 0.05 mg/kg BW buprenorphine (Indivior UK Limited, Slough, UK) followed by mechanical ventilation. As previously described,<sup>25</sup> a 1.2F micro-tip catheter (SciSense, Ontario, Canada) was used for continuous recording of LV pressure-volume loops. For volume correction, 5-10  $\mu$ L of 10% sodium chloride solution (Fresenius Kabi AG, Bad Homburg, Germany), were injected. To avoid the effect of artificial ventilation, data were always recorded at apnea. As indices for heart function, ejection fraction (EF; in %), LV maximum pressure ( $LVP_{max}$ ; in mmHg), maximal rate of LV pressure rise ( $dP/dt_{max}$ ; in mmHg/s), and maximal rate of LV pressure reduction ( $dP/dt_{min}$ ; in mmHg/s) were assessed.

### Sample collection

After the hemodynamic measurement, mice were euthanized under anesthesia via cervical dislocation, followed by

harvesting of the LV, which was immediately snap-frozen. Additionally, the spleen was harvested and stored on ice for splenocyte isolation.

### Immunohistochemistry

Frozen LV tissue samples were cut in 5 µm thick sections and used for immunohistological staining with the following antibodies directed against CCL2 (Abnova, Taipei, Taiwan, PAB16617, 1:25, overnight), CCL7 (Cloud clone corp., Katy, TX, USA, PAA089Mu01, 1:25, overnight), CX3CL1 (Abcam, Cambridge, UK, AB25088, 1:75), collagen I (Chemicon, Darmstadt, Germany, AB765P, 1:300) and CD68 (Abcam, Cambridge, UK, AB53444, 1:600).<sup>26</sup> Stained slides were investigated on a Leica DM2000 LED microscope (Leica Microsystems GmbH, Wetzlar, Germany) at a 100× magnification. The analysis was performed in a blinded fashion manner via digital image analysis using Leica Application Suite version 4.4 (LAS V4.4).

### Flow cytometry

Splenocytes were isolated from all groups, according to Van Linthout *et al.*<sup>9</sup> For the acute CVB3 myocarditis set, 1 pool of spleens from  $n = 3$  mice was generated for the control, CVB3, and CVB3 + RAA-CardAPs groups, whereas for CVB3 + EMB-CardAPs mice, 2 spleen pools of  $n = 2$  mice were generated. For the chronic CVB3 myocarditis sets, splenocytes were isolated from individual spleens. Pro-inflammatory and anti-inflammatory monocyte subsets were determined, as described previously.<sup>22,25</sup> Cells were stained at 4 °C for CD11b (PerCP/Cyanine5.5, 101228, 1:40), CD115 (Alexa488, 135524, 1:50), Ly6C (Brilliant Violet 421, 128032, 1:33), CCR2 (Alexa647, 150604, 1:50), and CX3CR1 (PE, 341604, 1:100) (all antibodies were purchased from BioLegend, Koblenz, Germany). Splenocytes were used for the analysis of Ly6C<sup>high</sup>CCR2<sup>high</sup>CX3CR1<sup>low</sup>, Ly6C<sup>mid</sup>CCR2<sup>high</sup>CX3CR1<sup>low</sup>, and Ly6C<sup>low</sup>CCR2<sup>low</sup>CX3CR1<sup>high</sup> monocyte subsets. All measurements were performed on a MACSQuant Analyzer (Miltenyi Biotec, Bergisch Gladbach, Germany) and were analyzed with the FlowJo software version 8.7 (FlowJo, Ashland, OR, USA).

### Co-culture of splenocytes with right atrial appendage- and endomyocardial biopsy-derived cardiac adherent proliferating cells

To examine the effect of RAA-CardAPs and EMB-CardAPs on monocyte differentiation, splenocytes of control and acute CVB3-infected mice were plated at a density of  $1 \times 10^6$  cells/well in Rosewell Park Memorial Institute 1640 medium (Thermo Fischer Scientific, Darmstadt, Germany) that was supplemented with 10% FBS (Biochrom, Berlin, Germany) and 1% penicillin/streptomycin (Biochrom, Berlin, Germany). Two hours after seeding, RAA-CardAPs and EMB-CardAPs were added at a ratio of 1:10 for 24 hours to splenocytes from CVB3-infected mice. Subsequently, splenocytes were stained at 4 °C for CD11b, CD115, Ly6C, CCR2, and CX3CR1 (all antibodies were purchased from BioLegend, Koblenz, Germany) and measured by flow cytometry (see above).

### Gene expression analysis

As previously described,<sup>19</sup> RNA was isolated from the LV using the RNeasy Mini Kit (Macherey Nagel, Düren, Germany) and subsequently reverse transcribed using the high-capacity cDNA kit (Applied Biosystems, Darmstadt, Germany). Quantitative real-time PCR was performed on a QuantStudio 6 Flex Real-Time PCR System (Thermo Fischer

Scientific, Darmstadt, Germany) to assess cardiac gene expression levels. To this end, the following commercially available gene expression assays (Applied Biosystems), were used: Chemokine (C-C motif) ligand (CCL) 2 (Mm00441242\_m1), CCL7 (Mm00443113\_m1), chemokine (C-X3-C motif) ligand (CX3CL) 1 (Mm00436454\_m1), intercellular adhesion molecule (ICAM)-1 (Mm00516023\_m1), interleukin (IL)-6 (Mm00446190\_m1), lysyl oxidase (LOX) (Mm00495386\_m1), tumor necrosis factor (TNF)- $\alpha$  (Mm00443258\_m1), and vascular cell adhesion molecule (VCAM)-1 (Mm01320970\_m1). Gene expression was normalized to the housekeeping gene glyceraldehyde-3-phosphate dehydrogenase (GAPDH, Mm99999915\_g1) and relatively expressed with the control group set as 1 using the  $2^{-\Delta\Delta C_t}$  method.<sup>27</sup>

### Myocarditis score

Hematoxylin/eosin (HE) staining was performed on 5 µm thick cryosections. A semiquantitative scale, with severity scores from 0 to 4 (0, no inflammatory infiltrates; 1, small foci of inflammatory cells between myocytes; 2, foci > 100 inflammatory cells; 3, larger foci with an area  $\leq 5\%$  of cross-section involved; 4, >5% of a cross-section involved), was used to quantify myocardial damage that comprised cardiac cell necrosis, inflammation, and scarring according to Savvatis and Van Linthout *et al.*<sup>14</sup> Analysis was performed in a blinded fashion manner via digital image analysis using Leica Application Suite version 4.4 (LAS V4.4).

### Statistical analysis

Statistical analysis was performed using Graph Pad Prism 9.5.1 for Windows 10 (GraphPad Software, La Jolla, USA). Data are represented as scatter plots with bars, showing individual data points and the corresponding mean  $\pm$  standard error of the mean. For normally distributed data, an ordinary 1-way analysis of variance with uncorrected Fisher's LSD post hoc test was performed. In case data were not normally distributed, Kruskal-Wallis test with corrected Dunn's post hoc test was performed.

## Results

### Right atrial appendage-derived cardiac adherent proliferating cells improve left ventricular function and reduce cardiac fibrosis in acute Coxsackievirus B3-induced myocarditis mice

To evaluate the cardioprotective and immunomodulatory effects of RAA-CardAPs, RAA-CardAPs were i.v. injected in the viral (d1 post CVB3 infection; Figure 1A) phase. EMB-CardAPs, known to exert cardioprotective effects in acute CVB3 C57BL/6J myocarditis mice,<sup>18</sup> were administered as reference cells. Six days after i.v. cell application, cardiac function was determined by pressure-volume loop measurements (Figure 1A-E). CVB3-infected mice exhibited impaired LV function (Figure 1C, F-I). RAA-CardAPs and EMB-CardAPs improved both parameters of systolic (LVP<sub>max</sub>, Figure 1G) and diastolic function (dP/dt<sub>min</sub>, Figure 1I) in CVB3 mice.

To evaluate the impact of RAA-CardAPs and EMB-CardAPs on cardiac fibrosis, immunohistochemistry of the main extracellular matrix protein collagen I<sup>9</sup> and real-time PCR of the crosslinking protein LOX were performed. LV collagen I deposition tended to be higher in CVB3 versus control mice, whereas LV LOX mRNA expression was increased in CVB3 versus control mice (Figure 1J and K). RAA- and EMB-CardAPs



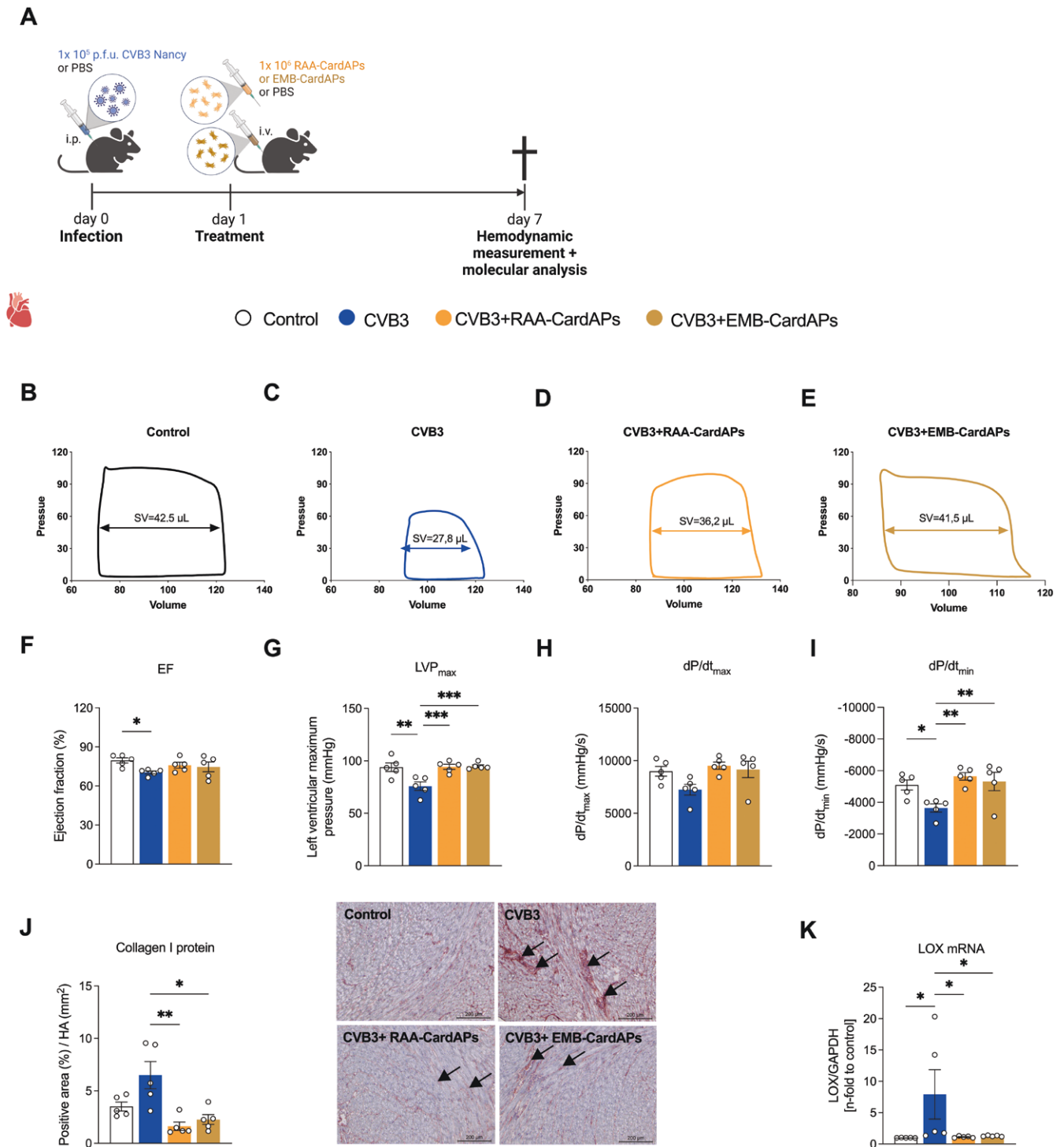


**Figure 1.** Right atrial appendage (RAA)-cardiac adherent proliferating cells (CardAPs) improve left ventricular function and reduce cardiac fibrosis in acute Coxsackievirus B3 (CVB3)-induced myocarditis mice. (A) Experimental design of the study. (B-E) Representative pressure-volume loops of Control and CVB3-infected mice injected with PBS (CVB3), RAA-CardAPs (CVB3 + RAA-CardAPs orange) or endomyocardial biopsy (EMB)-CardAPs (CVB3 + EMB-CardAPs), with indicated stroke volume (SV). (F-I) left ventricle (LV) function in control, CVB3, CVB3 + RAA-CardAPs and CVB3 + EMB-CardAPs mice, as indicated by (F) LV ejection fraction (EF; %), (G) LV maximum pressure (LVP<sub>max</sub>; mmHg), (H) dP/dt<sub>max</sub> (mmHg/s), and (I) dP/dt<sub>min</sub> (mmHg/s), respectively, which were obtained as indices of LV function by conductance catheter. (J-K) Cardiac fibrosis, as analyzed by LV (J) collagen I, depicted as positive area (%)/heart area (HA; mm<sup>2</sup>) (left panel). Representative pictures are shown in the respective right panel (magnification 100×, scale bar = 200 μm) with arrows indicating collagen I deposition, shown in red; and (K) LOX mRNA expression depicted as *n*-fold with control mice set as 1. Data are represented as scatter plots with bars, showing individual data points and the corresponding mean ± standard error of the mean (SEM). Statistical differences were assessed using 1-way analysis of variance (ANOVA) or Kruskal-Wallis test (\**P* < .05, \*\**P* < .01, and \*\*\**P* < .001, *n* = 5/group).

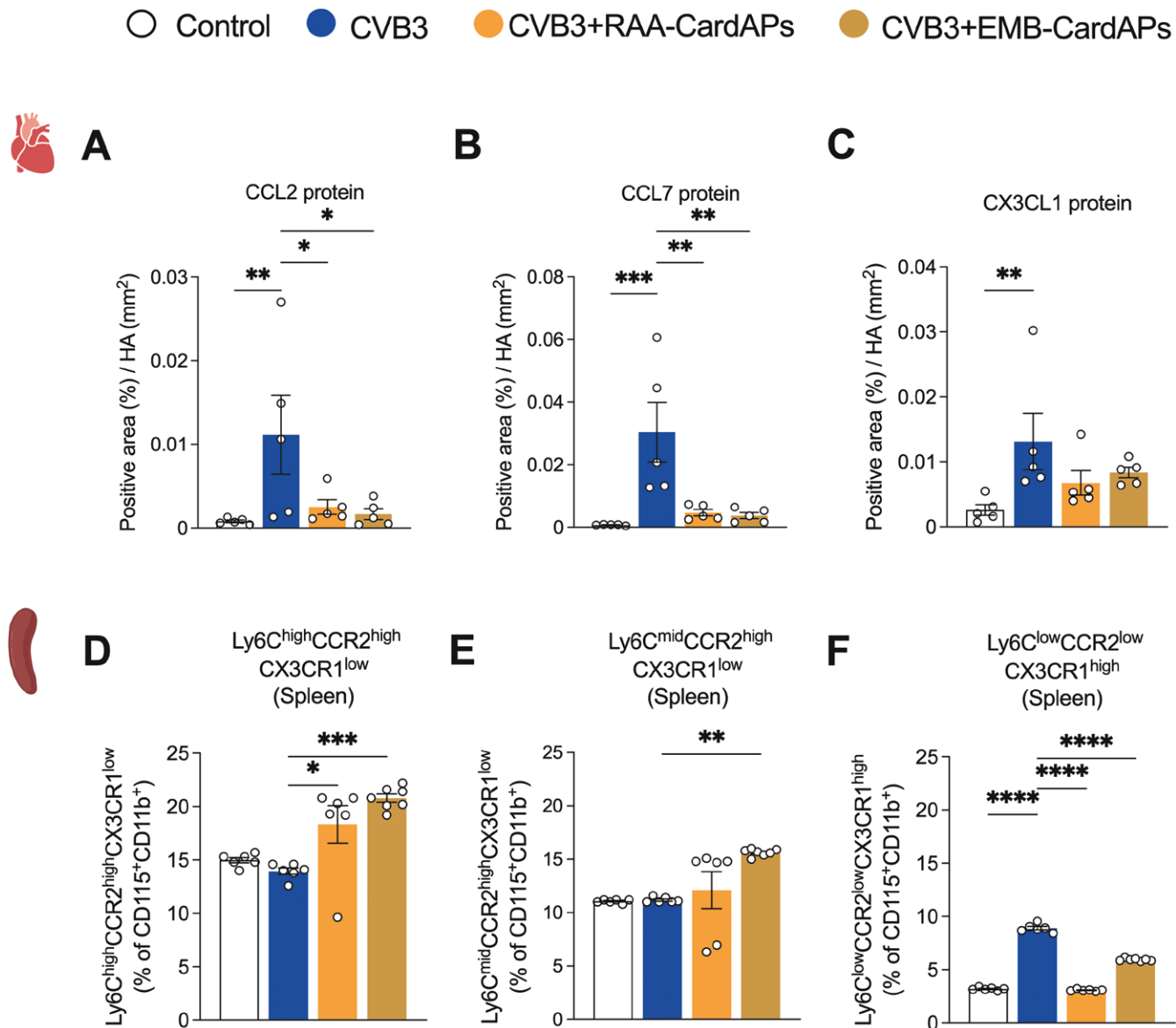


**Figure 2.** RAA-CardAPs modulate cardiac chemokine expression and splenic pro- and anti-inflammatory monocytes in acute CVB3-induced myocarditis mice. (A-E) The impact of RAA-CardAPs and EMB-CardAPs on LV protein expression of the chemokines CCL2 and CCL7 attracting pro-inflammatory monocytes, and CX3CL1, attracting anti-inflammatory monocytes in PBS-injected and CVB3-infected mice was analyzed via LV immunohistological stainings of (A) CCL2, (B) CCL7, (C) CX3CL1, depicted as positive area (%) / HA (mm<sup>2</sup>). (D-F) To determine the impact of RAA-CardAPs and EMB-CardAPs on splenic pro-inflammatory and anti-inflammatory monocytes, the percentage of (D) pro-inflammatory Ly6C<sup>high</sup>CCR2<sup>high</sup>CX3CR1<sup>low</sup> and (E) Ly6C<sup>mid</sup>CCR2<sup>high</sup>CX3CR1<sup>low</sup> of gated CD115<sup>+</sup>CD11b<sup>+</sup> and the percentage of (F) anti-inflammatory Ly6C<sup>low</sup>CCR2<sup>low</sup>CX3CR1<sup>high</sup> of gated CD115<sup>+</sup>CD11b<sup>+</sup> monocytes in the spleen was analyzed. Data are represented as scatter plots with bars, showing individual data points and the corresponding mean  $\pm$  SEM. Statistical differences were assessed using 1-way ANOVA or Kruskal-Wallis test (\* $P < .05$ , \*\* $P < .01$ , \*\*\* $P < 0.001$ , and \*\*\*\* $P < .0001$ ,  $n = 5$ /group for all analysis except for (D-F)  $n = 3$ -4/group).

application in CVB3 mice decreased LV collagen I expression by 4.0-fold ( $P < .01$ ) and 2.9-fold ( $P < .05$ ), respectively, which was accompanied by a 7.1-fold ( $P < .05$ ) and 6.2-fold ( $P < .05$ ) reduction of LV LOX mRNA expression compared to the PBS-treated CVB3 group, respectively (Figure 1J and K).

#### Right atrial appendage-derived cardiac adherent proliferating cells exert immunomodulatory effects in acute Coxsackievirus B3-induced myocarditis mice

Given the importance of monocytes as central mediators in myocarditis<sup>22,25,28</sup> and the relevance of the chemokines CCL2, CCL7 and CX3CL1 in the attraction of pro- and

anti-inflammatory monocytes to the heart in CVB3 myocarditis,<sup>25</sup> we next evaluated the impact of RAA-CardAPs on the LV expression of these chemokines. In agreement with Pappritz *et al.*,<sup>25</sup> CVB3 infection led to an upregulation in cardiac CCL2 and CCL7 protein expression versus control mice (Figure 2A and B). CX3CL1, known to attract anti-inflammatory Ly6C<sup>low</sup> monocytes into the myocardium in CVB3 myocarditis,<sup>22</sup> was also increased in CVB3-infected compared to control mice (Figure 2C). CVB3 + RAA-CardAPs and CVB3 + EMB-CardAPs mice exhibited lower CCL2 and CCL7 expression in comparison to CVB3-infected mice (Figure 2A and B). Consequently, CCL2/CX3CL1 and CCL7/CX3CL1 protein ratios tended to be lower in CVB3 + RAA-CardAPs

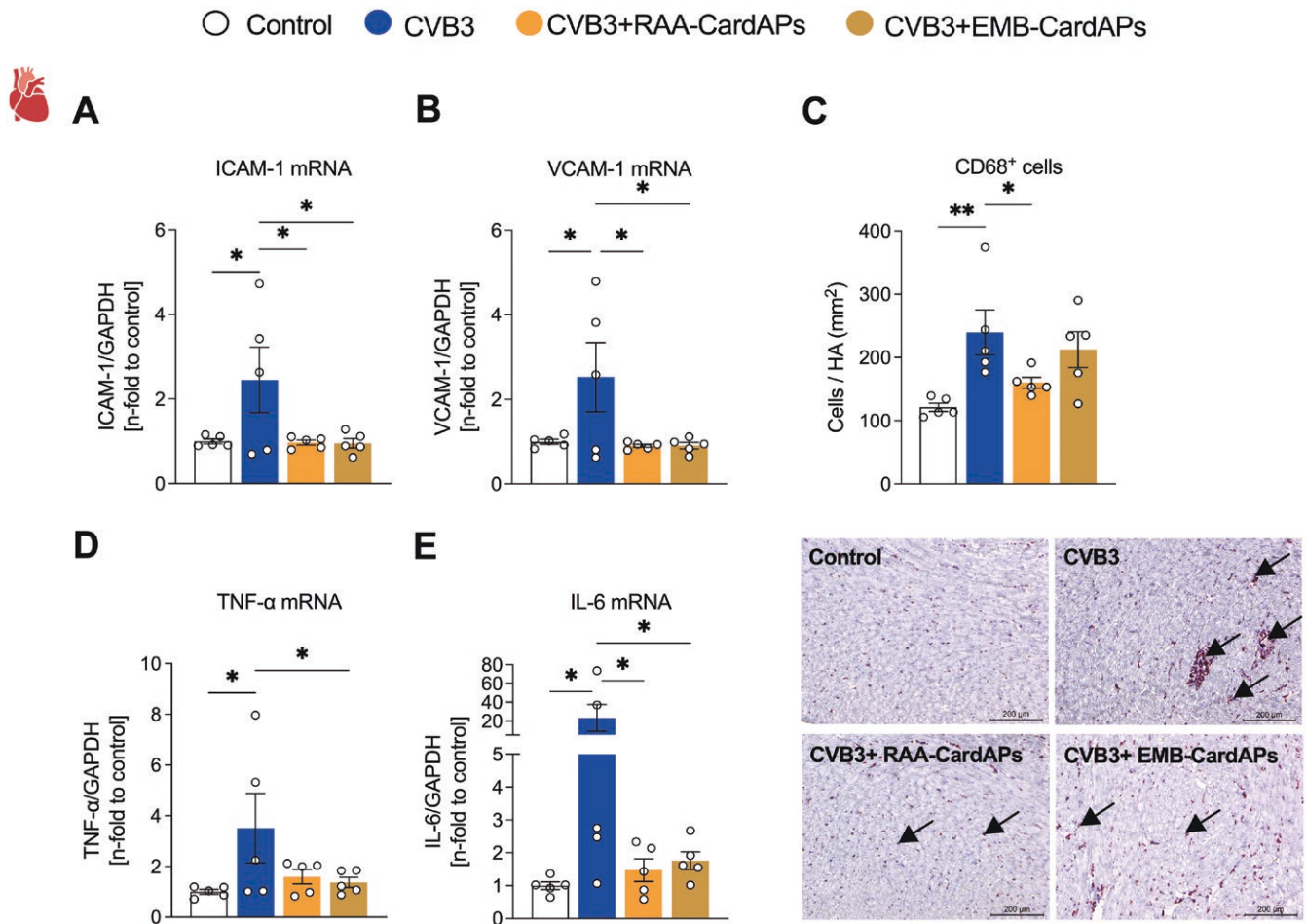


**Figure 3.** RAA-CardAPs reduce cardiac adhesion molecule expression, CD68<sup>+</sup> cell presence and cytokine expression in acute CVB3-induced myocarditis mice. (A and B) LV intercellular adhesion molecule (ICAM)-1 and vascular cell adhesion molecule (VCAM)-1 mRNA expression was determined via real-time PCR, with LV (A) ICAM-1 and (B) VCAM-1 mRNA expression depicted as *n*-fold with control mice set as 1. (C) LV presence of CD68<sup>+</sup> cells was analyzed via immunohistochemistry and depicted as number of cells/HA (mm<sup>2</sup>) (upper panel) with representative pictures shown in the lower panel (magnification 100 $\times$ , scale bar = 200  $\mu$ m) with arrows indicating CD68<sup>+</sup> cells. (D and E) Finally, LV mRNA expression of the cytokines TNF- $\alpha$  and IL-6 was analyzed via real-time PCR with (D) TNF- $\alpha$  and (E) IL-6 mRNA expression depicted as *n*-fold with control mice set as 1. Data are represented as scatter plots with bars, showing individual data points and the corresponding mean  $\pm$  SEM. Statistical differences were assessed using 1-way ANOVA (\* $P$  < .05 and \*\* $P$  < .01,  $n$  = 5/group for all analysis).

and CVB3 + EMB-CardAPs mice compared to untreated CVB3 mice (data not shown). With the spleen as the reservoir of monocytes, which migrate to the heart upon injury,<sup>1,22,29</sup> we next evaluated the impact of i.v. RAA-CardAPs and EMB-CardAPs application on splenic monocytes subsets.<sup>22</sup> Characterization of monocyte subsets by flow cytometry displayed no significant difference in the pro-inflammatory Ly6C<sup>high</sup>CCR2<sup>high</sup>CX3CR1<sup>low</sup> or Ly6C<sup>mid</sup>CCR2<sup>high</sup>CX3CR1<sup>low</sup> cells in spleens of CVB3 versus control mice (Figure 2D and E). However, CVB3 infection increased the splenic anti-inflammatory Ly6C<sup>low</sup>CCR2<sup>low</sup>CX3CR1<sup>high</sup> monocyte subset (Figure 2F). Treatment of CVB3 mice with RAA-CardAPs and EMB-CardAPs led to a higher percentage of pro-inflammatory Ly6C<sup>high</sup>CCR2<sup>high</sup>CX3CR1<sup>low</sup> cells in the spleen compared with CVB3 mice (Figure 2D). In addition, i.v. administration of RAA-CardAPs and EMB-CardAPs reduced the anti-inflammatory Ly6C<sup>low</sup>CCR2<sup>low</sup>CX3CR1<sup>high</sup> splenic cells of CVB3 mice, compared to untreated CVB3-infected mice (Figure 2F).

Giving the importance of adhesion molecules for monocytes adhesion and subsequent infiltration,<sup>22</sup> LV ICAM-1 and VCAM-1 mRNA expression was next evaluated.

CVB3-infected mice displayed 2.5-fold ( $P$  < .05) and 2.6-fold ( $P$  < .05) elevated LV ICAM-1 and VCAM-1 mRNA expression versus control mice (Figure 3A and B), respectively. Both RAA-CardAPs and EMB-CardAPs reduced LV ICAM-1 and VCAM-1 mRNA expression in CVB3 mice (Figure 3A and B). To evaluate the impact of RAA-CardAPs and EMB-CardAPs on the presence of cardiac monocytes/macrophages in CVB3-induced myocarditis, immunohistochemistry of CD68<sup>+</sup> cells on LV sections was performed. The analysis revealed a significant ( $P$  < .01) increase in the number of CD68<sup>+</sup> cells in the LV of CVB3-infected versus control mice (Figure 3C). RAA-CardAPs application reduced the number of CD68<sup>+</sup> cells in the LV compared to CVB3 mice by-fold ( $P$  < .05), whereas no differences in LV CD68<sup>+</sup> cells were found following EMB-CardAPs administration (Figure 3C). In parallel to the increased CD68<sup>+</sup> monocytes/macrophages presence, CVB3 mice exhibited elevated LV TNF- $\alpha$  and IL-6 mRNA levels compared to control mice (Figure 3D and E). RAA-CardAPs and EMB-CardAPs application in CVB3 mice reduced LV TNF- $\alpha$  or/and IL-6 mRNA expression compared to untreated CVB3 mice (Figure 3D and E), respectively.

### Right atrial appendage-derived cardiac adherent proliferating cells modulate monocyte differentiation in vitro

To assess whether the changes in splenic monocyte subsets observed in CVB3 + RAA-CardAPs and CVB3 + EMB-CardAPs mice compared with CVB3 mice were a result of the impact of RAA- and EMB-CardAPs on monocyte differentiation, splenocytes from acute CVB3-infected mice were co-cultured with isolated RAA-CardAPs and EMB-CardAPs, with monocultured splenocytes of CVB3 and control mice as reference. After 24 hours, splenic monocyte subsets were determined via flow cytometry (Figure 4A-C). Briefly, the percentage of pro-inflammatory  $\text{Ly6C}^{\text{high}}\text{CCR2}^{\text{high}}\text{CX3CR1}^{\text{low}}$  and  $\text{Ly6C}^{\text{mid}}\text{CCR2}^{\text{high}}\text{CX3CR1}^{\text{low}}$  subsets (Figure 4A and B) and anti-inflammatory  $\text{Ly6C}^{\text{low}}\text{CCR2}^{\text{low}}\text{CX3CR1}^{\text{high}}$  monocyte subset (Figure 4C) was higher in the CVB3 splenocytes compared to controls. Addition of RAA-CardAPs and EMB-CardAPs to CVB3 splenocytes reduced the percentage of pro-inflammatory  $\text{Ly6C}^{\text{high}}\text{CCR2}^{\text{high}}\text{CX3CR1}^{\text{low}}$  and  $\text{Ly6C}^{\text{mid}}\text{CCR2}^{\text{high}}\text{CX3CR1}^{\text{low}}$  subsets ( $P < .0001$ ) (Figure 4A and B), whereas only EMB-CardAPs decreased anti-inflammatory  $\text{Ly6C}^{\text{low}}\text{CCR2}^{\text{low}}\text{CX3CR1}^{\text{high}}$  monocyte subsets (Figure 4C).

### Right atrial appendage-derived cardiac adherent proliferating cells improve left ventricular function and reduce cardiac fibrosis in chronic Coxsackievirus B3-induced myocarditis mice

After assessing the cardioprotective and immunomodulatory effects of RAA-CardAPs following i.v. injection in the viral phase of acute CVB3 myocarditis mice, we next evaluated the impact of RAA-CardAPs i.v. administered in the inflammatory (d10 post CVB3 infection; Figure 5A) phase of chronic CVB3 NMRI myocarditis mice. Mice were hemodynamically characterized via conductance catheter 28d

after CVB3 infection and subsequently sacrificed (Figure 5A-E). Chronic CVB3 NMRI mice exhibited impaired LV systolic and diastolic function versus control mice (Figure 5C, F-I). RAA-CardAPs improved LV systolic function ( $\text{EF}$ :  $P < .01$ ;  $\text{LVP}_{\text{max}}$ :  $P = .058$  and  $\text{dP/dt}_{\text{max}}$ :  $P < .01$ ) and tended to improve diastolic function ( $\text{dP/dt}_{\text{min}}$ :  $P = .064$ ) when injected in the inflammatory phase of chronic CVB3 mice (Figure 5F-I). In line with these findings, LV collagen I protein level and LOX mRNA expression were increased in CVB3-infected mice compared to control mice, whereas RAA-CardAPs administration decreased LV collagen I expression, but did not affect LV LOX mRNA expression (Figure 5J and K).

### Right atrial appendage-derived cardiac adherent proliferating cells exert immunomodulatory effects in chronic Coxsackievirus B3-induced myocarditis mice

We next evaluated the immunomodulatory potential of RAA-CardAPs upon injection in the inflammatory phase of chronic CVB3 mice. In contrast to acute CVB3 mice, LV mRNA expression of the chemokines CCL2, CCL7, and CX3CL1 were not altered in chronic CVB3 versus control mice. Furthermore, no significant differences in LV CCL2, CCL7, and CX3CL1 mRNA expression were observed in the RAA-CardAPs-treated versus untreated CVB3 mice (Figure 6A-C). To determine the impact of RAA-CardAPs on the cardiac infiltrating monocyte subsets in CVB3-induced myocarditis, flow cytometry analysis of the splenic pro- and anti-inflammatory monocyte subsets was performed. The analysis revealed an increase in the percentage of pro-inflammatory  $\text{Ly6C}^{\text{high}}\text{CCR2}^{\text{high}}\text{CX3CR1}^{\text{low}}$  and  $\text{Ly6C}^{\text{mid}}\text{CCR2}^{\text{high}}\text{CX3CR1}^{\text{low}}$  monocytes in CVB3-infected versus control mice (Figure 6D-F). RAA-CardAPs application reduced the percentage of splenic  $\text{Ly6C}^{\text{mid}}\text{CCR2}^{\text{high}}\text{CX3CR1}^{\text{low}}$  monocytes compared

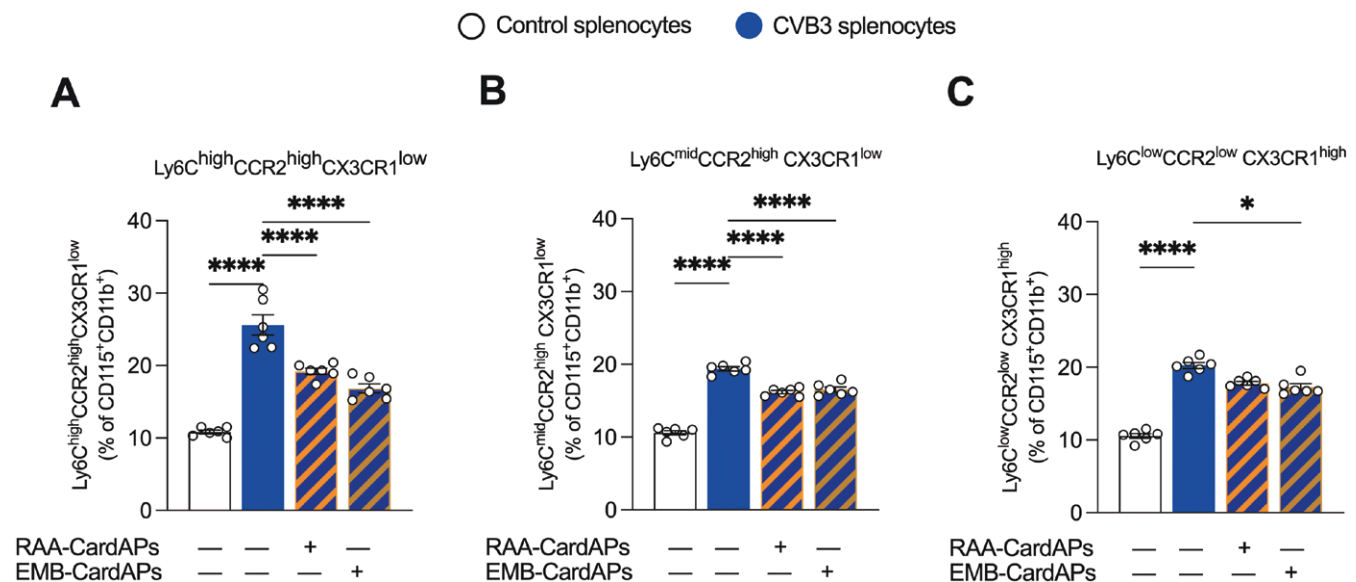


**Figure 4.** RAA-CardAPs modulate monocyte differentiation in vitro. The impact of RAA-CardAPs and EMB-CardAPs on splenic monocyte differentiation was evaluated in vitro. Therefore, splenocytes from acute CVB3-infected mice were co-cultured with isolated RAA-CardAPs and EMB-CardAPs, with monocultured splenocytes of CVB3 and control mice as reference. After 24 hours, splenocytes were collected and the percentage of pro-inflammatory (A)  $\text{Ly6C}^{\text{high}}\text{CCR2}^{\text{high}}\text{CX3CR1}^{\text{low}}$  and (B)  $\text{Ly6C}^{\text{mid}}\text{CCR2}^{\text{high}}\text{CX3CR1}^{\text{low}}$  and of anti-inflammatory (C)  $\text{Ly6C}^{\text{low}}\text{CCR2}^{\text{low}}\text{CX3CR1}^{\text{high}}$  of gated  $\text{CD115}^+\text{CD11b}^+$  monocytes was analyzed. Data are represented as scatter plots with bars, showing individual data points and the corresponding mean  $\pm$  SEM. Statistical differences were assessed using 1-way ANOVA or Kruskal-Wallis test (\* $P < .05$  and \*\*\*\* $P < .0001$ ,  $n = 6/\text{group}$ ).



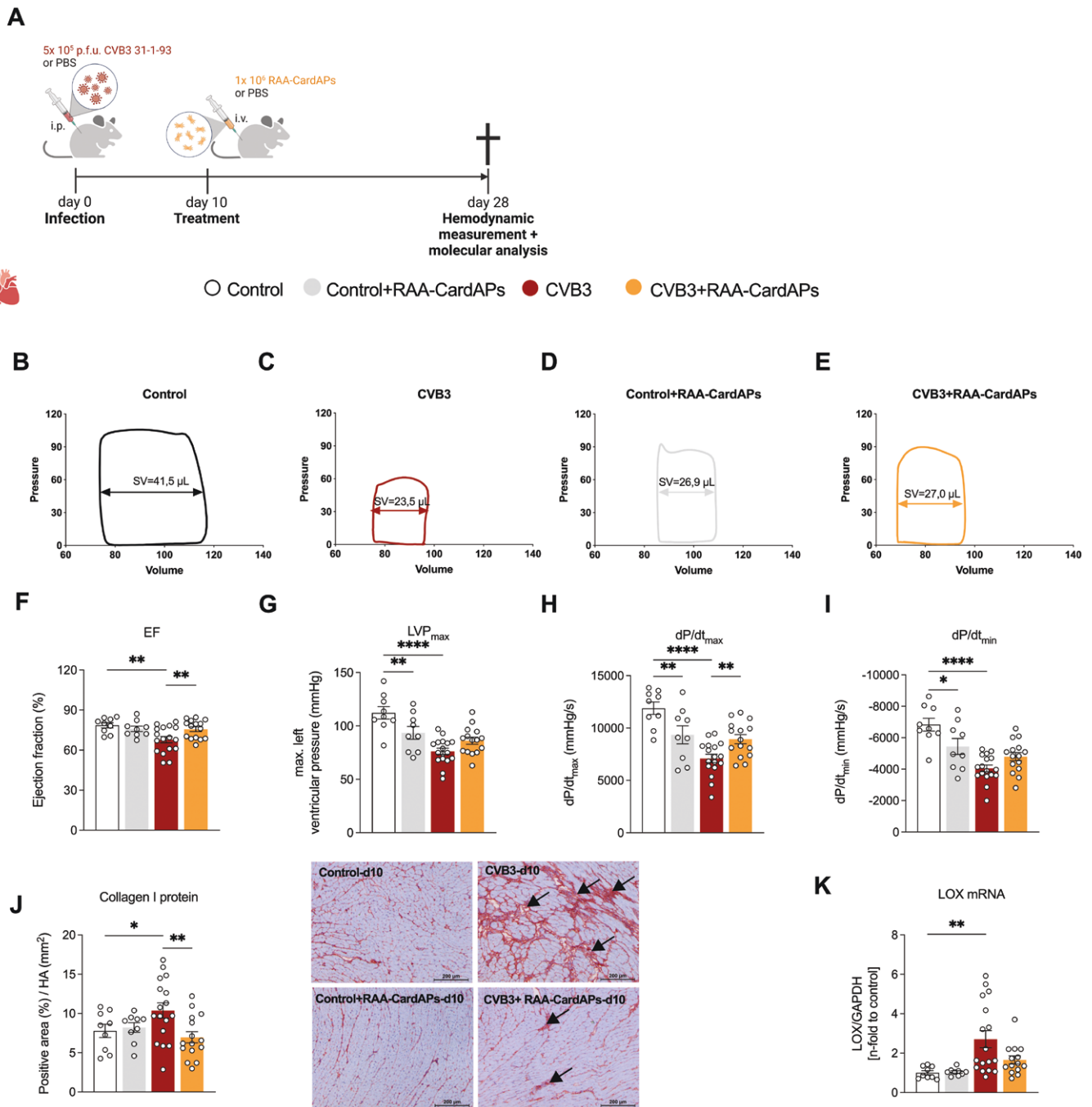


**Figure 5.** RAA-CardAPs improve left ventricular function and reduce cardiac fibrosis in chronic CVB3-induced myocarditis mice. (A) Experimental design of the study. (B-E) Representative pressure-volume loops of Control mice injected with PBS (Control) or RAA-CardAPs (Control + RAA-CardAPs) and CVB3-infected mice injected with PBS (CVB3) or RAA-CardAPs at d10 after CVB3 infection (CVB3 + RAA-CardAPs), with indicated SV. (F-I) LV function in Control, Control + RAA-CardAPs, CVB3 or CVB3 + RAA-CardAPs mice, as indicated by (F) LV EF (%), (G) LV maximum pressure (LVP<sub>max</sub>; mmHg), (H) dP/dt<sub>max</sub> (mmHg/s), and (I) dP/dt<sub>min</sub> (mmHg/s), respectively, which were obtained as indices of LV function by conductance catheter. (J) Left panel: LV collagen I in mice injected with PBS or RAA-CardAPs at d10 after CVB3 infection, was analyzed via immunohistochemical stainings and depicted as positive area (%) / HA (mm<sup>2</sup>). Right panel: collagen I-stained sections (magnification 100 $\times$ , scale bar = 200  $\mu$ m) with arrows indicating collagen I deposition; and (K) LOX mRNA expression depicted as *n*-fold with control mice set as 1. Data are represented as scatter plots with bars, showing individual data points and the corresponding mean  $\pm$  SEM. Statistical differences were assessed using 1-way ANOVA or Kruskal-Wallis test (\**P* < .05, \*\**P* < .01, and \*\*\*\**P* < .0001, F-K: *n* = 9/Control and Control + RAA-CardAPs, *n* = 15-17/CVB3 and CVB3 + RAA-CardAPs).

to CVB3 mice (Figure 6E). With respect to the anti-inflammatory monocyte subset Ly6C<sup>low</sup>CCR2<sup>low</sup>CX3CR1<sup>high</sup>, RAA-CardAPs-treated CVB3 mice exhibited a lower percentage of anti-inflammatory splenic Ly6C<sup>low</sup>CCR2<sup>low</sup>CX3CR1<sup>high</sup> monocyte subset versus CVB3 mice (Figure 6F).

Strikingly, RAA-CardAPs increased the percentage of pro-inflammatory splenic Ly6C<sup>high</sup>CCR2<sup>high</sup>CX3CR1<sup>low</sup> and Ly6C<sup>mid</sup>CCR2<sup>high</sup>CX3CR1<sup>low</sup> monocytes and reduced the percentage of the anti-inflammatory monocyte-subset Ly6C<sup>low</sup>CCR2<sup>low</sup>CX3CR1<sup>high</sup> in control mice.

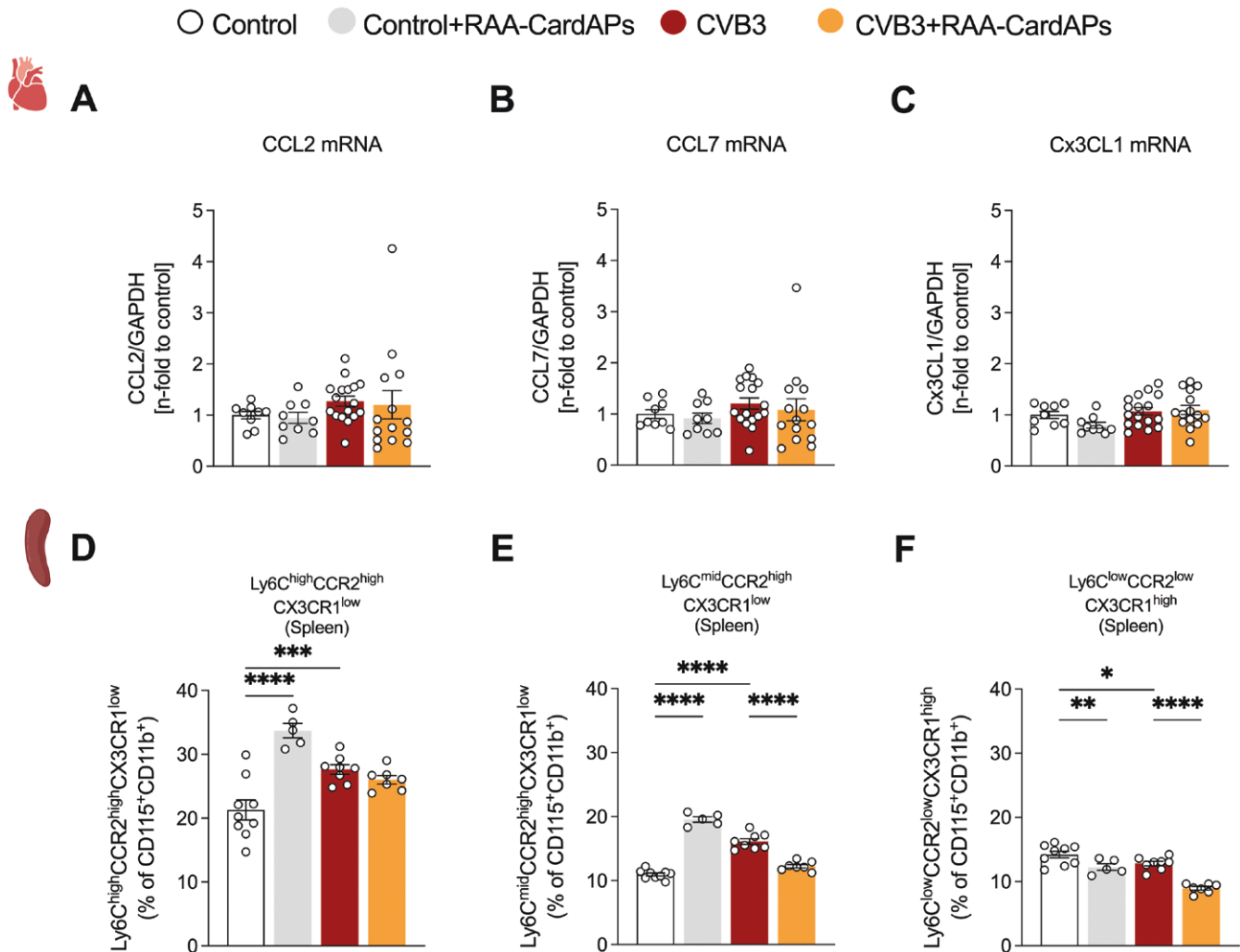


**Figure 6.** RAA-CardAPs decrease splenic pro-inflammatory monocytes in chronic CVB3-induced myocarditis mice. (A-C) LV mRNA expression of the chemokines CCL2, CCL7, and CX3CL1 was analyzed via real-time PCR with (A) CCL2, (B) CCL7, and (C) CX3CL1 mRNA expression depicted as  $n$ -fold with control mice set as 1. (D-F) The impact of RAA-CardAPs injected at d10 post CVB3 infection on splenic pro-inflammatory and anti-inflammatory monocytes was evaluated. Therefore, the percentage of (D) pro-inflammatory  $Ly6C^{high}CCR2^{high}CX3CR1^{low}$  and (E)  $Ly6C^{mid}CCR2^{high}CX3CR1^{low}$  of gated  $CD115^{+}CD11b^{+}$  and the percentage of (F) anti-inflammatory  $Ly6C^{low}CCR2^{low}CX3CR1^{high}$  of gated  $CD115^{+}CD11b^{+}$  monocytes in the spleen was analyzed. Data are represented as scatter plots with bars, showing individual data points and the corresponding mean  $\pm$  SEM. Statistical differences were assessed using 1-way ANOVA or Kruskal-Wallis test (\* $P < .05$ , \*\* $P < .01$ , \*\*\* $P < .001$ , and \*\*\*\* $P < .0001$ , (A-C)  $n = 9$ /Control and Control + RAA-CardAPs,  $n = 14$ -17/CVB3, and CVB3 + RAA-CardAPs, (D-F)  $n = 5$ -9/group).

LV ICAM-1 and VCAM-1 mRNA expression was next evaluated. CVB3-infected mice CVB3 mice exhibited 1.6-fold ( $P < .0001$ ) and 1.9-fold ( $P < .0001$ ) elevated LV ICAM-1 and VCAM-1 mRNA levels versus control mice (Figure 7A and B), respectively, with no changes after RAA-CardAPs application. The myocarditis score was significantly lower in the chronic CVB3 mice treated with RAA-CardAPs compared to untreated CVB3 mice (Figure 7C) and RAA-CardAP cells tended to reduce the upregulated presence of  $CD68^{+}$  cells ( $P = .11$ ) in the LV of chronic CVB3-induced myocarditis mice (Figure 7D). In line with the rise in  $CD68^{+}$  monocytes/macrophages, CVB3 mice exhibited elevated LV IL-6 mRNA levels compared to control mice (Figure 7F). Though, RAA-CardAPs did not affect LV TNF- $\alpha$ , nor LV IL-6 mRNA expression in CVB3 mice.

## Discussion

In this study, we show that i.v. application of RAA-CardAPs leads to systemic and cardiac immunomodulation,

accompanied with a reduction of cardiac fibrosis, and reflected in an improvement in LV function in murine acute and chronic CVB3-induced myocarditis

Despite increasing knowledge in the pathogenesis of CVB3-induced myocarditis, no target-specific treatment options are available or have failed due to detrimental effects.<sup>30</sup> At end-stage heart failure, only heart transplantation can be performed,<sup>1</sup> indicating the demand for new treatment options. In this regard, cell-based therapy might be a promising option to overcome this gap.<sup>9,18,25</sup> EMB-CardAPs provide favorable conditions for the treatment of acute CVB3 myocarditis, given their immunomodulatory and anti-fibrotic properties.<sup>18,19</sup> Though, a disadvantage of EMB-CardAPs is the limited cell number, which can be generated from 1 EMB. This hurdle has been overcome by using the RAA instead of EMB as cell source, allowing allogeneic and off-the-shelf use, the latter being another important asset in view of application into a clinical condition as acute myocarditis. With modulation of the cardiosplenic axis, ie, the homing of monocytes from

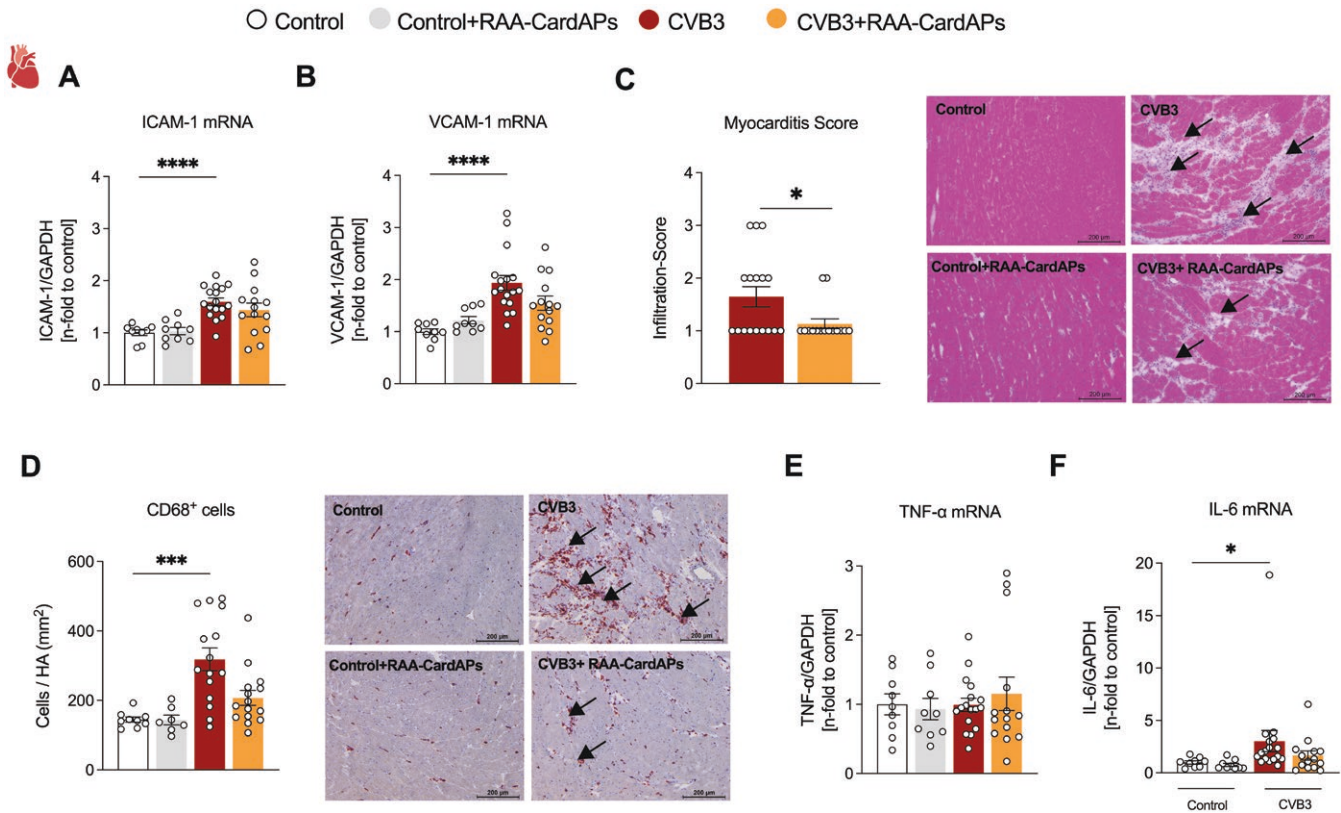


**Figure 7.** RAA-CardAPs reduce the severity of myocarditis in chronic CVB3-induced myocarditis mice. (A and B) Next, LV mRNA expression of intercellular and vascular adhesion molecules was determined via real-time PCR, with LV (A) ICAM-1 and (B) VCAM-1 mRNA expression depicted as *n*-fold with control mice set as 1. (C) Left panel: The myocarditis score of mice injected with PBS or RAA-CardAPs at d10 after CVB3 infection. The severity scores from 0 to 4 (0, no inflammatory infiltrates; 1, small foci of inflammatory cells between myocytes; 2, foci > 100 inflammatory cells; 3, larger foci with an area ≤5% of cross-section involved; 4, >5% of a cross-section involved). Right panel: hematoxylin/eosin (HE)-stained sections (magnification 100×, scale bar = 200 μm) with arrows indicating regions of cell infiltrates, cell necrosis, and scarring. (D) Left panel: LV presence of CD68<sup>+</sup> cells in control or CVB3-infected mice injected with PBS or RAA-CardAPs at d10 after CVB3 infection, was analyzed via immunohistochemical stainings and depicted as number of cells/HA (mm<sup>2</sup>). Right panel: Representative images of CD68 immunostainings (magnification 100×, scale bar = 200 μm) with arrows indicating CD68<sup>+</sup> cells. Finally, LV mRNA expression of the cytokines TNF-α and IL-6 was analyzed via real-time PCR with (E) TNF-α and (F) IL-6 mRNA expression depicted as *n*-fold with control mice set as 1. Data are represented as scatter plots with bars, showing individual data points and the corresponding mean ± SEM. Statistical differences were assessed using 1-way ANOVA, Kruskal-Wallis test, or Mann Whitney t-test (\**P* < .05, \*\**P* < .01, \*\*\**P* < .001, and \*\*\*\**P* < .0001, *n* = 9/Control and Control + RAA-CardAPs, *n* = 15-17/CVB3, and CVB3 + RAA-CardAPs).

the spleen towards the heart and their involvement in subsequent cardiac remodeling, being an attractive therapeutic approach to treat myocarditis,<sup>28</sup> the impact of i.v. RAA-CardAPs administration on CVB3 acute myocarditis was investigated. Evaluation of the effects of i.v. RAA-CardAPs application in CVB3 mice, using EMB-CardAPs as reference cell, showed decreased LV expression of the chemokines CCL2 and CCL7, known to attract pro-inflammatory monocytes.<sup>31</sup> In parallel, CVB3 + RAA-CardAPs mice tended to exhibit a lower LV CCL2/CX3CL1 and CCL7/CX3CL1 chemokine ratios in CVB3-infected mice. With CX3CL1/fractalkine, being responsible for the recruitment of anti-inflammatory monocytes into the myocardium,<sup>22</sup> these findings suggest an enhanced migration of anti-inflammatory monocytes towards the heart. This hypothesis was further built on own previous findings by which an increase in anti-inflammatory Ly6C<sup>low</sup>CCR2<sup>low</sup>CX3CR1<sup>high</sup> cells was found in the heart, paralleled by their drop in the spleen of CVB3 mice after Treg injection.<sup>25</sup> In frame with this hypothesis, a decrease in anti-inflammatory Ly6C<sup>low</sup>CCR2<sup>low</sup>CX3CR1<sup>high</sup> cells was observed in the spleen of CVB3 + RAA-CardAPs

and CVB3 + EMB-CardAPs versus CVB3 mice. In parallel, RAA-CardAPs and EMB-CardAPs reduced LV mRNA levels of the adhesion molecules ICAM-1 and VCAM-1, which are of relevance for monocyte adhesion and subsequent infiltration into the insulted cardiac tissue.<sup>22</sup> Immunohistochemistry further illustrated a decline in the presence of cardiac CD68<sup>+</sup> monocytes/macrophages in CVB3 + RAA-CardAPs versus CVB3 mice. Whereas this effect was not found in CVB3 + EMB-CardAPs mice, modulation of cardiac pro-versus anti-inflammatory monocytes following EMB-CardAPs may not be excluded, neither a reduction in mononuclear cell activation, as previously shown following EMB-CardAPs administration in CVB3 mice.<sup>18</sup> The above mentioned findings together with the observation that supplementation of both RAA-CardAPs and EMB-CardAPs to splenocytes from CVB3 mice reduced the percentage of pro-inflammatory monocytes compared to monocultured splenocytes from CVB3 mice further speculates lower enrichment of pro-inflammatory monocytes in the hearts of both CVB3 + RAA-CardAPs and CVB3 + EMB-CardAPs mice compared with CVB3 mice. Despite the limitation of the study not directly showing a



correlation between splenic monocyte phenotypes and cardiac monocyte infiltration, lower LV mRNA expression of the pro-inflammatory cytokine IL-6 was shown in both CVB3 + RAA-CardAPs and CVB3 + EMB-CardAPs compared with CVB3 mice. This supports the presence of less pro-inflammatory monocytes in the LV of CVB3 mice following RAA-CardAPs and EMB-CardAPs application and is further in line with the feature that both EMB-CardAPs<sup>18</sup> and RAA-CardAPs<sup>21</sup> are primed by the inflammatory environment in exerting their immunomodulatory effects.

Progression of viral myocarditis is attributed to the inflammatory response, which can develop to alterations in the ECM and cardiac fibrosis leading to deterioration in cardiac function.<sup>32,33</sup> In agreement with the previously shown anti-fibrotic potential of EMB-CardAPs,<sup>19</sup> administration of RAA-CardAPs and EMB-CardAPs attenuated collagen deposition, as indicated by the decreased LV collagen I protein level and the reduced LV expression of the crosslinking enzyme LOX in acute CVB3-induced myocarditis. Several studies have demonstrated the specific contribution of monocytes/macrophages on the modulation of cardiac fibroblasts and subsequent cardiac function.<sup>28,29</sup> Migration of anti-inflammatory Ly6C<sup>low</sup>CCR2<sup>low</sup>CX3CR1<sup>high</sup> monocytes to the heart, and the turnover to macrophages, have been proposed to reduce myocardial fibrosis and prevent myocarditis.<sup>34</sup> In this regard, we postulate that the anti-fibrotic effects observed following RAA-CardAPs and EMB-CardAPs in CVB3 mice can be partially explained via their immunomodulatory effects on the monocyte subset. Though, a direct anti-fibrotic effect on cardiac fibroblasts as previously shown for EMB-CardAPs cannot be excluded.<sup>19</sup>

Since in patients there is a gap between CVB3 infection and occurrence of first symptoms, early treatment with RAA-CardAPs after CVB3 infection as successfully done in acute CVB3 myocarditis mice may not always be possible. Therefore, we also investigated the therapeutic potential of RAA-CardAPs in chronic CVB3 myocarditis mice injected at a later time point, ie, at d10 post CVB3 infection, in the inflammatory phase. RAA-CardAPs administration at d10 post CVB3 infection resulted in improved LV function, less cardiac damage and fibrosis. The therapeutic benefit from RAA-CardAPs following injection in the inflammatory phase is underbuilt by the fact that RAA-CardAPs<sup>21</sup> similar to EMB-CardAPs<sup>18</sup> and MSC<sup>9</sup> are primed by their inflammatory environment. This hypothesis is further supported by the finding that RAA-CardAPs injected at d10 reverted the CVB3-mediated modulation of pro-inflammatory monocytes in the spleen, but at the other hand increased pro-inflammatory monocytes in the spleen paralleled by an impairment in LV function parameters in control mice.

The abovementioned findings related to the administration of RAA-CardAPs in the inflammatory phase of chronic myocarditis are of translational value, not solely for RAA-CardAPs, but for immunomodulatory strategies in general. It accentuates the importance of the therapy window and of the target patient collective. Despite the limitation that in the chronic model only RAA-CardAPs and no EMB-CardAPs were evaluated, the latter is supported by recent findings by which mesenchymal precursor cell therapy in patients with heart failure with reduced EF was the most effective in patients with evidence of systemic inflammation (high-sensitivity C-reactive protein levels  $\geq 2$  mg/L).<sup>13</sup>

## Conclusion

In conclusion, RAA-CardAPs exert immunomodulatory effects, reduce cardiac inflammation, cardiac fibrosis, and the development of cardiac dysfunction in CVB3-infected mice. These findings further support the concept that modulation of the cardiosplenic axis is an attractive therapeutic approach to treat myocarditis. Overall, our study shows the therapeutic efficacy of i.v. RAA-CardAPs application for acute and chronic CVB3 myocarditis.

## Acknowledgements

The authors would like to acknowledge the assistance of the BCRT Flow Cytometry Lab and Fengquan Dong, Annika Koschel, Jie Lin, Kerstin Puhl, and Marzena Sosnowski (in alphabetical order) for their excellent technical support. This work was supported by the Berlin-Brandenburg Center for Regenerative Therapies—BCRT (Bundesministerium für Bildung und Forschung—0313911) to M.H., Mi.S., C.T., and S.V.L. Open Access funding was enabled and organized by Projekt DEAL.

## Author contributions

M.El-Shafeey: Investigation, Formal analysis, Writing - original draft; K.P.: Investigation, Formal analysis; I.V.: Formal analysis, Visualization; Writing - review & editing; K.M.: Investigation, Formal analysis; A.A.: Formal analysis; M.Seifert: Formal analysis; H.F.: Resources, Investigation, Formal analysis; J.K.: Supervision; K.K.: Investigation, Formal analysis; M.H. Resources; M.Sittinger: Resources; C.T.: Resources, Data curation, Writing - review & editing; S.V.L.: Conceptualization, Formal analysis, Data curation, Supervision, Funding acquisition, Writing - original draft, Writing - review & editing.

## Funding

This work was supported by the Berlin-Brandenburg Center for Regenerative Therapies—BCRT (Bundesministerium für Bildung und Forschung—0313911) to M.H., Mi.S., C.T., and S.V.L. Open Access funding was enabled and organized by Projekt DEAL.

## Conflicts of interest

M.S. is a shareholder of CellServe GmbH (Berlin, Germany) and BioRetis GmbH (Berlin, Germany). CellServe owns a license for CardAP cells. M.H., M.S., and C.T. are investors of patent EP000002129774A1 “Cells for heart treatment.” The remaining authors report no competing financial interests.

## Data availability

The data that support the findings of this study are available from the corresponding author upon reasonable request.

## References

1. Tschope C, Ammirati E, Bozkurt B, et al. Myocarditis and inflammatory cardiomyopathy: current evidence and future directions. *Nat Rev Cardiol.* 2021;18:169-193. <https://doi.org/10.1038/s41569-020-00435-x>



2. Heymans S, Van Linthout S, Kraus SM, Cooper LT, Ntusi NAB. Clinical characteristics and mechanisms of acute myocarditis. *Circ Res.* 2024;135:397-411. <https://doi.org/10.1161/CIRCRESAHA.124.324674>
3. Van Linthout S, Tschöpe C. Viral myocarditis: a prime example for endomyocardial biopsy-guided diagnosis and therapy. *Curr Opin Cardiol.* 2018;33:325-333. <https://doi.org/10.1097/HCO.0000000000000515>
4. Burch GE, Sun SC, Chu KC, Sohal RS, Colcolough HL. Interstitial and coxsackievirus B myocarditis in infants and children. A comparative histologic and immunofluorescent study of 50 autopsied hearts. *JAMA.* 1968;203:1-8.
5. Golpour A, Patriki D, Hanson PJ, McManus B, Heidecker B. Epidemiological impact of myocarditis. *J Clin Med* 2021;10:603. <https://doi.org/10.3390/jcm10040603>
6. Tschöpe C, Cooper LT, Torre-Amione G, Van Linthout S. Management of myocarditis-related cardiomyopathy in adults. *Circ Res.* 2019;124:1568-1583. <https://doi.org/10.1161/CIRCRESAHA.118.313578>
7. Braunwald E. Cell-based therapy in cardiac regeneration: an overview. *Circ Res.* 2018;123:132-137. <https://doi.org/10.1161/CIRCRESAHA.118.313484>
8. Fuentes T, Kearns-Jonker M. Endogenous cardiac stem cells for the treatment of heart failure. *Stem Cells Cloning* 2013;6:1-12. <https://doi.org/10.2147/SCCAA.S29221>
9. Van Linthout S, Savvatis K, Miteva K, et al. Mesenchymal stem cells improve murine acute coxsackievirus B3-induced myocarditis. *Eur Heart J.* 2011;32:2168-2178. <https://doi.org/10.1093/eurheartj/ehq467>
10. Kinnaird T, Stabile E, Burnett MS, et al. Local delivery of marrow-derived stromal cells augments collateral perfusion through paracrine mechanisms. *Circulation.* 2004;109:1543-1549. <https://doi.org/10.1161/01.CIR.0000124062.31102.57>
11. Gnecci M, He H, Liang OD, et al. Paracrine action accounts for marked protection of ischemic heart by Akt-modified mesenchymal stem cells. *Nat Med.* 2005;11:367-368. <https://doi.org/10.1038/nm0405-367>
12. Wysoczynski M, Khan A, Bolli R. New paradigms in cell therapy: repeated dosing, intravenous delivery, immunomodulatory actions, and new cell types. *Circ Res.* 2018;123:138-158. <https://doi.org/10.1161/CIRCRESAHA.118.313251>
13. Perin EC, Borow KM, Henry TD, et al. Randomized trial of targeted transendocardial mesenchymal precursor cell therapy in patients with heart failure. *J Am Coll Cardiol* 2023;81:849-863. <https://doi.org/10.1016/j.jacc.2022.11.061>
14. Haag M, van Linthout S, Miteva K, et al. Mesenchymal stromal cells but not cardiac fibroblasts exert beneficial systemic immunomodulatory effects in experimental myocarditis. *PLoS One.* 2012;7:e41047. <https://doi.org/10.1371/journal.pone.0041047>
15. Madonna R, Van Laake LW, Botker HE, et al. ESC Working Group on Cellular Biology of the Heart: position paper for Cardiovascular Research: tissue engineering strategies combined with cell therapies for cardiac repair in ischaemic heart disease and heart failure. *Cardiovasc Res.* 2019;115:488-500. <https://doi.org/10.1093/cvr/cvz010>
16. Haag M, Van Linthout S, Schröder SE, et al. Endomyocardial biopsy derived adherent proliferating cells - a potential cell source for cardiac tissue engineering. *J Cell Biochem.* 2010;109:564-575. <https://doi.org/10.1002/jcb.22433>
17. Haag M, Stolk M, Ringe J, et al. Immune attributes of cardiac-derived adherent proliferating (CAP) cells in cardiac therapy. *J Tissue Eng Regen Med.* 2013;7:362-370. <https://doi.org/10.1002/term.531>
18. Miteva K, Haag M, Peng J, et al. Human cardiac-derived adherent proliferating cells reduce murine acute Coxsackievirus B3-induced myocarditis. *PLoS One.* 2011;6:e28513. <https://doi.org/10.1371/journal.pone.0028513>
19. Miteva K, Van Linthout S, Pappritz K, et al. Human endomyocardial biopsy specimen-derived stromal cells modulate angiotensin II-induced cardiac remodeling. *Stem Cells Transl. Med.* 2016;5:1707-1718. <https://doi.org/10.5966/sctm.2016-0031>
20. Detert S, Stamm C, Beez C, et al. The atrial appendage as a suitable source to generate cardiac-derived adherent proliferating cells for regenerative cell-based therapies. *J Tissue Eng Regen Med.* 2018;12:e1404-e1417. <https://doi.org/10.1002/term.2528>
21. Diedrichs F, Stolk M, Jurchott K, et al. Enhanced immunomodulation in inflammatory environments favors human cardiac mesenchymal stromal-like cells for allogeneic cell therapies. *Front Immunol.* 2019;10:1716. <https://doi.org/10.3389/fimmu.2019.01716>
22. Miteva K, Pappritz K, El-Shafeey M, et al. Mesenchymal stromal cells modulate monocytes trafficking in coxsackievirus B3-induced myocarditis. *Stem Cells Transl. Med.* 2017;6:1249-1261. <https://doi.org/10.1002/sctm.16-0353>
23. Miteva K, Pappritz K, Sosnowski M, et al. Mesenchymal stromal cells inhibit NLRP3 inflammasome activation in a model of Coxsackievirus B3-induced inflammatory cardiomyopathy. *Sci Rep.* 2018;8:2820. <https://doi.org/10.1038/s41598-018-20686-6>
24. Pinkert S, Dieringer B, Klopffleisch R, et al. Early treatment of coxsackievirus B3-infected animals with soluble coxsackievirus-adenovirus receptor inhibits development of chronic coxsackievirus B3 cardiomyopathy. *Circ Heart Fail* 2019;12:e005250. <https://doi.org/10.1161/CIRCHEARTFAILURE.119.005250>
25. Pappritz K, Savvatis K, Miteva K, et al. Immunomodulation by adoptive regulatory T-cell transfer improves Coxsackievirus B3-induced myocarditis. *FASEB J.* 2018;32(11):fj201701408R. <https://doi.org/10.1096/fj.201701408R>
26. Savvatis K, Müller I, Fröhlich M, et al. Interleukin-6 receptor inhibition modulates the immune reaction and restores titin phosphorylation in experimental myocarditis. *Basic Res Cardiol.* 2014;109:449. <https://doi.org/10.1007/s00395-014-0449-2>
27. Livak KJ, Schmittgen TD. Analysis of relative gene expression data using real-time quantitative PCR and the 2(-Delta Delta C(T)) Method. *Methods.* 2001;25:402-408. <https://doi.org/10.1006/meth.2001.1262>
28. Leuschner F, Courties G, Dutta P, et al. Silencing of CCR2 in myocarditis. *Eur Heart J.* 2015;36:1478-1488. <https://doi.org/10.1093/eurheartj/ehu225>
29. Peet C, Ivetic A, Bromage DI, Shah AM. Cardiac monocytes and macrophages after myocardial infarction. *Cardiovasc Res.* 2020;116:1101-1112. <https://doi.org/10.1093/cvr/cvz336>
30. Van Linthout S, Tschöpe C, Schultheiss HP. Lack in treatment options for virus-induced inflammatory cardiomyopathy: can iPS-derived cardiomyocytes close the gap? *Circ Res.* 2014;115:540-541. <https://doi.org/10.1161/CIRCRESAHA.114.304951>
31. Shi C, Pamer EG. Monocyte recruitment during infection and inflammation. *Nat Rev Immunol.* 2011;11:762-774. <https://doi.org/10.1038/nri3070>
32. Van Linthout S, Miteva K, Tschöpe C. Crosstalk between fibroblasts and inflammatory cells. *Cardiovasc Res.* 2014;102:258-269. <https://doi.org/10.1093/cvr/cvu062>
33. Tschöpe C, Van Linthout S, Jäger S, et al. Modulation of the acute defence reaction by eplerenone prevents cardiac disease progression in viral myocarditis. *ESC Heart Failure* 2020;7:2838-2852. <https://doi.org/10.1002/ehf2.12887>
34. Hou X, Chen G, Bracamonte-Baran W, et al. The cardiac microenvironment instructs divergent monocyte fates and functions in myocarditis. *Cell Rep* 2019;28:172-189.e7. <https://doi.org/10.1016/j.celrep.2019.06.007>